



EFFECT OF N-BUTANOL ADDITION ON SOOT FORMATION OF N-HEPTANE IN A MICRO FLOW REACTOR WITH A CONTROLLED TEMPERATURE PROFILE

Mohd Hafidzal Bin Mohd Hanafi¹, Hisashi Nakamura¹, Takuya Tezuka¹ and Kaoru Maruta^{1,2}

¹Institute of Fluid Science, Tohoku University, 2-1-1 Katahira, Aoba, Sendai, Japan

²ICE Lab., Far Eastern Federal University, Russky Island, Vladivostok, Russia

E-Mail: hafidzal@edyn.ifs.tohoku.ac.jp

ABSTRACT

The effect of *n*-butanol addition on the sooting limit of *n*-heptane was studied by using a micro flow reactor with a controlled temperature profile. Pure *n*-heptane and *n*-butanol + *n*-heptane (10:90) were employed in this study. The experiments were conducted for various equivalence ratios, $\phi = 1.5 - 3.5$. The inlet mean velocity was $U_0 = 10$ cm/s, maximum wall temperature was 1300 K under atmospheric pressure condition. The results showed three types of flame and soot responses: flame, flame with soot and only soot. In addition, the experimental results showed that the presence of *n*-butanol extended the sooting limit. Pure *n*-heptane showed soot starting to form at $\phi = 1.6$ whereas for 10% additional *n*-butanol, it started at $\phi = 1.9$. As the equivalence ratio, ϕ increases, experimental results showed more soot moving to lower temperatures. Computational results also showed Pyrene, A4 mole fraction increased as the equivalence ratio increases. Furthermore, soot was formed in a range of 1200 K to 1300 K. At higher equivalence ratios (3 and 3.5), experiments showed similar starting point of soot at lower temperature for pure *n*-heptane and blended fuel with 10% mole percentage addition of *n*-butanol. Computational A4 mole fraction was slightly decreased when 10% of *n*-butanol was introduced to the *n*-heptane. In computational results, a large difference in A4 mole fraction was shown between higher equivalence ratio (3.0 and 3.5) and lower equivalence ratio (1.5 to 2.0). Further study on chemical reactions focusing on A4 reaction is necessary in order to accurately describe the tendency of soot formation.

Keywords: soot formation, oxygenated fuel, micro combustor.

1. INTRODUCTION

Butanol is a second generation biofuel that is produced by a fermentation process of feed stocks. The molecular weight of butanol is 74.12 g/mole that is higher than methanol (32.04 g/mole) and ethanol (46.06 g/mole) due to the number of carbon atoms in their molecular structure. This gives butanol higher kinematic viscosity, energy density, good intersolubility with conventional fossil fuel without any cosolvent and produce a better fuel economy. Since saturation pressure for butanol is low, it causes a higher boiling point that contribute to lower volatility and self ignition which means that butanol has less possibility of vapor lock and cavitation in fuel supply systems compared to methanol and ethanol. Compared to diesel, volatility of butanol is higher which enhances combustion control.

Due to these advantages, researchers have investigated butanol combustion characteristics by experiments like jet stirred reactors [1][2], burner [3][4][5], and shock tubes [6][7]. Meanwhile, kinetic mechanism studies have been also done by [1][2][6][8][9][10].

Furthermore, most of the applications of butanol studies in engine proved that one of the significant advantage of butanol is the reduction of soot formation [11][12][13]. The study on the reduction of soot formation is important since it can contribute to adverse health effects and damage to the combustion cylinder in the engine. One of the approaches is by using butanol as an oxygenated fuel. Regarding the conditions of soot formation, previous researchers like Picket *et al.* [14]

pointed out that high temperatures (more than 1400 K or 1600 K), ignition delay time and amount of fuel were the three factors that influenced soot formation in premixed, partially premixed and diffusion flames. Wang *et al.* [15] also showed by using 2-D spray sooting flame simulations for *n*-heptane and *n*-butanol blended fuels, that local temperature higher than 1800 K is required for soot formation. In spite of a number of these studies, the effect of *n*-butanol on soot formation and the difference in sooting limits that occur at lower temperatures are still not well understood.

In this study, a micro flow reactor with a controlled temperature profile is introduced. The micro flow reactor consists of a quartz tube with an inner diameter smaller than the ordinary quenching diameter. An external heat source is employed to provide a stationary wall temperature profile along the flow direction. The flow inside the tube was laminar and at constant atmospheric pressure. Therefore, combustion and ignition characteristics of given fuels can be investigated in the well-defined experimental conditions.

The micro flow reactor was previously used to investigate general ignition characteristics of various fuels. Based on the inlet mean velocity, three types of flames which are normal flame, flame with repetitive extinction and ignition (FREI) and weak flame were identified [16][17][18][19]. By using the weak flames, general ignition properties of given fuels can be investigated. In addition to the general ignition characteristics, the determination of soot formation characteristics for different fuels and the formation



process of polycyclic aromatic hydrocarbons (PAH) were also successfully elucidated by the micro flow reactor [20][21]. Various types of flame and soot responses which depend on the equivalence ratio and the inlet mean velocity were investigated. PAH measurements and computations enable to validate and modify existing chemical kinetics for PAH formations.

In the present study, the same apparatus is employed in order to examine the sooting behavior and the effect of *n*-butanol addition to *n*-heptane on the sooting limits..

2. EXPERIMENTAL SETUP

a) Micro flow reactor with a controlled temperature profile

Schematics of the experimental setup is shown in Figure-1. The present study used a quartz tube with an inner diameter of 2 mm as a reactor. An H_2 /air burner was applied as an external heat source which created a stationary temperature profile along the inner surface of the quartz tube. The wall temperature of the inner surface along the axis of the quartz tube was measured using a K-type thermocouple that was inserted from the outlet of the tube. In this study, a temperature profile increasing from 340 K to 1300 K under atmospheric pressure were employed. This wall temperature was also employed in the computations and will be discussed later.

n-Butanol (>99.0% purity) and *n*-heptane (>99.0% purity) that obtained from Wako Pure Chemical Industries, Ltd. were employed in the present study. *n*-Butanol was selected as a representative of oxygenated fuels, while the selection of *n*-heptane was based on the fact that it is one of the primary reference fuels (PRF). Liquid fuel was supplied with a 500 μ L micro syringe (Hamilton 1750RN) that was installed with a stepping motor to control the fuel supply. Blended fuels were mixed in a liquid state to attain mole percentage in the gas phase for *n*-butanol + *n*-heptane (10:90).

The experiments were conducted at different equivalence ratios, ϕ within 1.5 - 4.5 and the inlet mean velocity, U_0 was 10 cm/s.. An electric heater that covered the upstream region was used in order to control the air temperature to vaporize the fuel before entering the reactor. A mass flow controller was used to control the rate of air flow. A digital still camera (Nikon D300) was used in order to capture the flame and soot images.

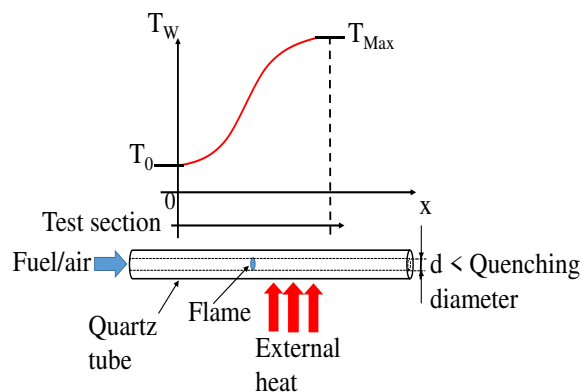


Figure-1. Schematics of the micro flow reactor with a controlled temperature profile.

b) Computational method

One-dimensional reactive steady flow computations based on PREMIX [22] with heat convection between the gas phase and the wall [16] by CHEMKIN-PRO were carried out. The experimental wall temperature profile from 340 K to 1300 K was employed in the heat convection term with a constant Nusselt number, ($Nu = 4$ for a constant heat flux [17]) for the energy equation [16] as shown in equation 1:

$$\dot{M} \frac{dT}{dX} - \frac{1}{c_p} \frac{d}{dx} \left(\lambda A \frac{dT}{dX} \right) + \frac{A}{c_p} \sum_{k=1}^K \rho Y_k V_k C_{pk} \frac{dT}{dX} + \frac{A}{c_p} \sum_{k=1}^K \dot{\omega}_k h_k W_k - \frac{A}{c_p} \frac{4\lambda Nu}{d^2} (T_w - T) = 0 \quad (1)$$

where \dot{M} , ρ , C_p , λ , d and A are mass flow rate, density, heat capacity at constant pressure, thermal conductivity, the inner diameter of the reactor and cross sectional area, respectively. Y_k , V_k , C_{pk} , $\dot{\omega}_k$, h_k and W_k are mass fraction, diffusion velocity, heat capacity at constant pressure, rate of production, enthalpy and molecular weight of species k , respectively. The same types of fuel, and pressure were employed as in the experimental conditions. A reduced kinetic model for *n*-heptane-*n*-butanol-PAH mechanism (76 species and 349 reactions) that was developed by Wang *et al.* [15] called Wang mechanism was employed in the computational. This mechanism is a combination of three parts which are primary reference fuel (PRF) mechanisms that were developed by Ra and Reitz [23], PAH mechanism by Slavinskaya *et al.* [24] and a reduced *n*-butanol mechanism developed by Sarathy *et al.* [1]. Wang mechanism considers the PAH growth up to pyrene, (A4) which is in good agreement with soot prediction. This mechanism also shows a good agreement with experimental results in shock tubes, constant volume chambers and testbed engine data.

We have focused on the mole fraction of pyrene ($C_{16}H_{10}$) called A4, since A4 is a soot inceptor in polycyclic aromatic hydrocarbons (PAHs) which is correlated to the prediction of soot formation [15]. Note that A4 mole fraction from the computational results is not



soot, however A4 mole fraction can be interpreted as a prediction of soot formation qualitatively.

3. RESULTS AND DISCUSSION

Figure-2 shows direct images of flame and soot responses for *n*-heptane and blended fuels. Three types of flame and soot formations were observed; flame, flame with soot formation and soot formation without flame.

Figure-3 summarizes the sooting limits behavior comparison of pure *n*-heptane and blended fuel of *n*-butanol + *n*-heptane (10:90). All results are plotted with respect to the equivalence ratio, ϕ (1.5 to 4.5) and with $U_0 = 10 \text{ cm/s}$. The variation of flame and soot responses is shown by different symbols and colors: blue triangles are only flame, green squares are flame and soot and red circles are soot only. The sooting limit is significantly increased when *n*-butanol is added to *n*-heptane. Soot starts to form at $\phi = 1.9$ and above for 10% of *n*-butanol addition, while for pure *n*-heptane, it is from $\phi = 1.6$ and above. The increase of the *n*-butanol fraction causes the sooting limit region to shift to higher equivalence ratios. Therefore, soot reduction obviously is achieved by the presence of *n*-butanol.

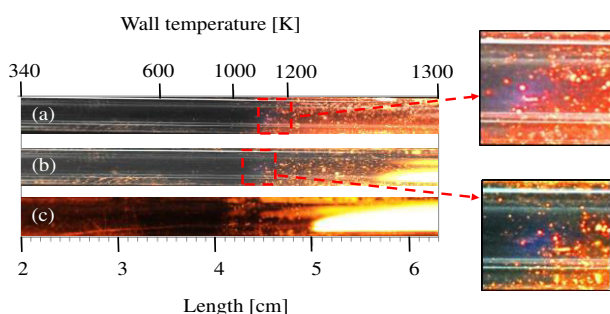


Figure-2. Direct images of flame and soot responses for: (a) *n*-butanol + *n*-heptane (10:90), flame: ($\phi = 1.8$); (b) *n*-butanol + *n*-heptane (10:90), flame + soot: ($\phi = 2$); (c) pure *n*-heptane, soot: ($\phi = 3.5$).

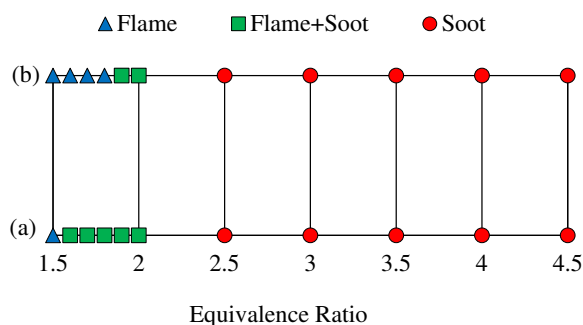


Figure-3. Flame and soot responses: (a) pure *n*-heptane, (b) *n*-butanol + *n*-heptane (10:90).

As mentioned before, pyrene (A4) is a soot precursor in PAH and it is treated as an indicator for sooting tendency. This is because soot is formed when large PAHs grow and integrate to form a solid particle.

Therefore, prediction of soot formation can be done by investigating A4 mole fraction from computations.

Figure-4 shows experimental and computational results for pure *n*-heptane. The experimental results (upper side) show soot formation is observed at the temperature range between 1200 K to 1300 K which is lower compared to previous researchers [14][15]. Soot begins to form at $\phi = 1.6$ and above. It can be seen that soot starts to rise from high temperatures and moves towards lower temperature as the equivalence ratio increases. In addition at higher ϕ , (3.0 to 3.5), the starting points of soot at lower temperatures is similar. In the computational results (lower side), Figure-4 also show that an increase of the equivalence ratio causes an increase of A4 mole fraction. A large difference in A4 mole fraction between lower ϕ , (1.5 to 2.0) and higher ϕ , (3.0 and 3.5) was observed.

Figure-5 shows experimental and computational results for an addition of 10% butanol. The experimental results (upper side) show soot formation is observed at the similar temperature range with that seen in Figure-4. Furthermore, computations (lower side) in Figure-5 also show a large difference between lower ϕ and higher ϕ . The influence of 10 % *n*-butanol addition on the soot formation and A4 mole fraction are shown in Figure-5. Soot formation in the micro flow reactor is substantially decreased with the addition of *n*-butanol to *n*-heptane by experiments. Soot does not appear at low equivalence ratios below $\phi = 1.9$ which shows the effect of *n*-butanol addition on the sooting limit (see Figure-3).

Addition of *n*-butanol also affects to the A4 mole fraction in the computation as shown in Figure-5. Figure 4 shows that the maximum computational A4 mole fraction at $\phi = 2$, for pure *n*-heptane is 4.2×10^{-9} . On the other hand, after the introduction of 10% of *n*-butanol, the maximum computational A4 mole fraction is decreased to 3.8×10^{-9} as shown in Figure-5. These computational results support the experimental findings regarding soot reduction through *n*-butanol addition.

However, the comparison between Figure-4 and Figure-5 for computational results of A4 mole fraction and experimental results of soot formation at $\phi = 1.6$ to 1.9 does not show a good agreement. The tendency for soot formation given by the maximum A4 mole fraction is not correlated with soot formation at $\phi = 1.6$ to 1.9. Therefore, the present study indicates that further improvements on chemical reaction mechanisms that focus on A4 reaction are needed.

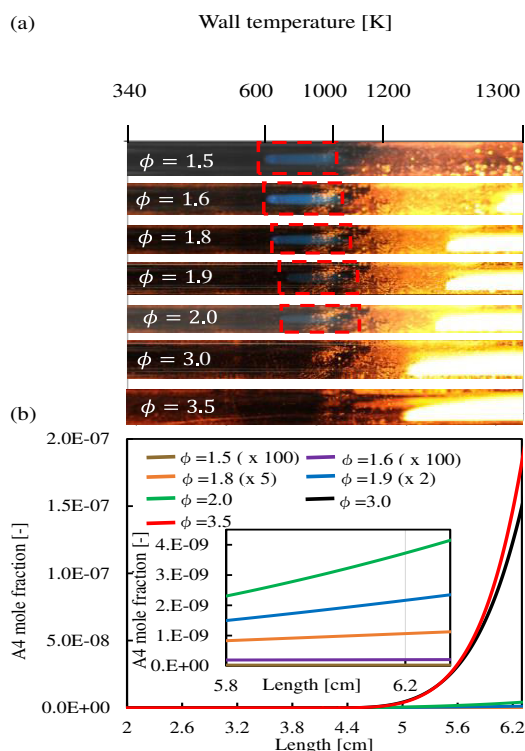


Figure-4. Direct images and A4 mole fraction for pure *n*-heptane. (a) Experimental results (b) Computational results.

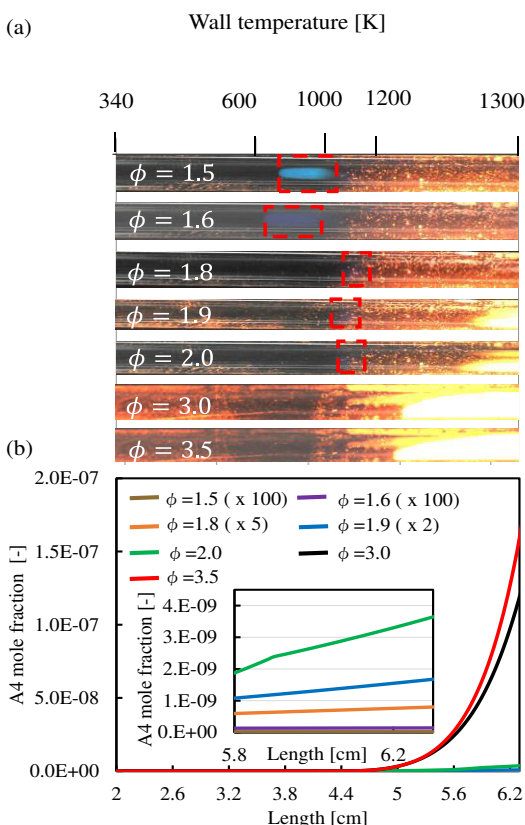


Figure-5. Direct images and A4 mole fraction for *n*-butanol + *n*-heptane (10:90). (a) Experimental results (b) Computational results.

4. CONCLUSIONS

This study was carried out in order to investigate the effect of *n*-butanol addition on the sooting limit of *n*-heptane in a micro flow reactor with a controlled temperature profile. For experimental results, three types of flame and soot responses could be observed: flame, flame with soot formation and soot formation without flame. The presence of *n*-butanol extended the sooting limit. For pure *n*-heptane, soot was observed from equivalence ratio, 1.6 and above meanwhile for 10% mole percentage addition of *n*-butanol, soot is observed from equivalence ratio, 1.9 and above. Computational A4 mole fraction which is a soot precursor is decreased when *n*-butanol is introduced to the *n*-heptane. In addition, regions of soot formation were observed in a temperature range around 1200 K to 1300K. As the equivalence ratio increased, more soot moves to lower temperature in the experimental results and computational A4 mole fraction also increased. For higher equivalence ratios (3 and 3.5), experimental results show similar starting point of soot at lower temperature for pure *n*-heptane and blended fuel with a 10% addition of *n*-butanol. Furthermore, in the computational results show that a large difference in A4 mole fraction between lower equivalence ratio (1.5 to 2) and higher equivalence ratio (3 to 3.5). Since this tendency does not fully support the experimental results, detailed examination on chemical reactions that focusing on A4 concentration is required in the future. In addition, it is indicated that the micro flow reactor can be applied in order to examine the effect of *n*-butanol on the soot formation under small difference of equivalence ratio.

ACKNOWLEDGEMENTS

The author would like to acknowledge Faculty of Mechanical Engineering, Universiti Teknikal Malaysia Melaka, Malaysia (UTeM).

REFERENCES

- [1] S. M. Sarathy, M. J. Thomson, C. Togbé, P. Dagaut, F. Halter, and C. Mounaim-Rousselle. 2009. An experimental and kinetic modeling study of *n*-butanol combustion. *Combustion and Flame*, 156(4): 852–864.
- [2] P. Dagaut, S. M. Sarathy, and M. J. Thomson. 2009. A chemical kinetic study of *n*-butanol oxidation at elevated pressure in a jet stirred reactor. *Proceedings of the Combustion Institute*, 32(1):229–237.
- [3] H. Ghiassi, P. Toth, and J. S. Lighty. 2014. Sooting behaviors of *n*-butanol and *n*-dodecane blends. *Combustion and Flame*, 161(3):671–679.
- [4] P. S. Veloo and F. N. Egolfopoulos. 2011. Flame propagation of butanol isomers/air mixtures. *Proc. Combust. Inst.*, 33(1):987–993.



- [5] J. Camacho, S. Lieb, and H. Wang. 2013. Evolution of size distribution of nascent soot in n- and i-butanol flames. *Proceedings of the Combustion Institute*, 34(1):1853–1860.
- [6] G. Black, H. J. Curran, S. Pichon, J. M. Simmie, and V. Zhukov. 2010. Bio-butanol: Combustion properties and detailed chemical kinetic model. *Combustion and Flame*, 157(2):363–373.
- [7] A. S. AlRamadan, J. Badra, T. Javed, M. Al-Abbad, N. Bokhumseen, P. Gaillard, H. Babiker, A. Farooq, and S. M. Sarathy. 2015. Mixed butanols addition to gasoline surrogates: Shock tube ignition delay time measurements and chemical kinetic modeling. *Combustion and Flame*, 162(10):3971–3979.
- [8] Frassoldati, R. Grana, T. Faravelli, E. Ranzi, P. Oßwald, and K. Kohse-Höinghaus. 2012. Detailed kinetic modeling of the combustion of the four butanol isomers in premixed low-pressure flames. *Combustion and Flame*, 159(7):2295–2311.
- [9] S. M. Sarathy, S. Vranckx, K. Yasunaga, M. Mehl, P. Oßwald, W. K. Metcalfe, C. K. Westbrook, W. J. Pitz, K. Kohse-Höinghaus, R. X. Fernandes, and H. J. Curran. 2012. A comprehensive chemical kinetic combustion model for the four butanol isomers. *Combustion and Flame*, 159(6):2028–2055.
- [10] R. Grana, A. Frassoldati, T. Faravelli, U. Niemann, E. Ranzi, R. Seiser, R. Cattolica, and K. Seshadri. 2010. An experimental and kinetic modeling study of combustion of isomers of butanol. *Combustion and Flame*, 157(11):2137–2154.
- [11] Q. Zhang, M. Yao, Z. Zheng, H. Liu, and J. Xu. 2012. Experimental study of n-butanol addition on performance and emissions with diesel low temperature combustion. *Energy*, 47(1):515–521.
- [12] M. Yao, H. Wang, Z. Zheng, and Y. Yue. 2010. Experimental study of n-butanol additive and multi-injection on HD diesel engine performance and emissions. *Fuel*, 89(9):2191–2201.
- [13] O. Doğan. 2011. The influence of n-butanol/diesel fuel blends utilization on a small diesel engine performance and emissions. *Fuel*, 90(7):2467–2472.
- [14] L. M. Pickett and D. L. Siebers. 2006. Soot Formation in Diesel Fuel Jets Near the Lift-Off Length. *Int. J. Engine Res.*, 7(2):103–130.
- [15] H. Wang, R. Deney Reitz, M. Yao, B. Yang, Q. Jiao, and L. Qiu. 2013. Development of an n-heptane-n-butanol-PAH mechanism and its application for combustion and soot prediction. *Combustion and Flame*, 160(3):504–519.
- [16] K. Maruta, T. Kataoka, N. Il Kim, S. Minaev, and R. Fursenko. 2005. Characteristics of combustion in a narrow channel with a temperature gradient. *Proceedings of the Combustion Institute*, 30(2):2429–2436.
- [17] M. Hori, H. Nakamura, T. Tezuka, S. Hasegawa, and K. Maruta. 2013. Characteristics of n-heptane and toluene weak flames in a micro flow reactor with a controlled temperature profile. *Proceedings of the Combustion Institute*, 34:3419–3426.
- [18] Y. Kizaki, H. Nakamura, T. Tezuka, S. Hasegawa, and K. Maruta. 2015. Effect of radical quenching on CH₄/air flames in a micro flow reactor with a controlled temperature profile. *Proceedings of the Combustion Institute*, 35(3):3389–3396.
- [19] S. Kikui, T. Kamada, H. Nakamura, T. Tezuka, S. Hasegawa, and K. Maruta. 2015. Characteristics of n-butane weak flames at elevated pressures in a micro flow reactor with a controlled temperature profile. *Proceedings of the Combustion Institute*, 35(3):3405–3412.
- [20] H. Nakamura, S. Suzuki, T. Tezuka, S. Hasegawa, and K. Maruta. 2015. Sooting limits and PAH formation of n-hexadecane and 2,2,4,4,6,8,8-heptamethylnonane in a micro flow reactor with a controlled temperature profile. *Proceedings of the Combustion Institute*, 35:3397–3404.
- [21] H. Nakamura, R. Tanimoto, T. Tezuka, S. Hasegawa, and K. Maruta. 2014. Soot formation characteristics and PAH formation process in a micro flow reactor with a controlled temperature profile. *Combustion and Flame*, 161:582–591.
- [22] J. A. M. R.J. Kee, J.F. Grcar, M.D. Smooke. 1985. A program for modeling steady, laminar, one-dimensional premixed flames. A Fortran Progr. Model. Steady Laminar One-dimensional Premixed Flames, Rep. No. SAND85-8240, Sandia Natl. Lab.
- [23] Y. Ra and R. D. Reitz. 2008. A reduced chemical kinetic model for IC engine combustion simulations with primary reference fuels. *Combustion and Flame*, 155(4):713–738.
- [24] N. a. Slavinskaya, U. Riedel, S. B. Dworkin, and M. J. Thomson. 2012. Detailed numerical modeling of PAH formation and growth in non-premixed ethylene and ethane flames. *Combustion and Flame*, 159(3):979–995.